ELSEVIER

Cement & Concrete Composites 26 (2004) 777–786

Cement & Concrete Composites

www.elsevier.com/locate/cemconcomp

Effectiveness of stirrups and steel fibres as shear reinforcement

Calogero Cucchiara, Lidia La Mendola *, Maurizio Papia

Dipartimento di Ingegneria Strutturale e Geotecnica, Universitá di Palermo, Viale delle Scienze, I90128 Palermo, Italy

Received 5 August 2002; accepted 14 July 2003

Abstract

This paper presents the results of experimental tests carried out on rectangular simply supported beams made of hooked steel fibre reinforced concrete with and without stirrups, subjected to two-point symmetrically placed vertical loads. The tests, carried out with controlled displacements, allow one to record complete load–deflection curves by means of which it is possible to deduce information on dissipative capacity and ductile behaviour up to failure. Depending on the amount of transverse reinforcement, volume fraction of fibres added in the mix and shear span, the collapse mechanism is due to predominant shear or flexure, thus showing the influence of the aforementioned structural parameters on the load carrying capacity and the post-peak behaviour of the beam. In particular, the results show that the inclusion of fibres in adequate percentage can change the brittle mode of failure characterizing shear collapse into a ductile flexural mechanism, confirming the possibility of achieving analogous performance by using reinforcing fibres instead of increasing the amount of transverse reinforcement. The ultimate values of the shear stresses recorded experimentally are compared with the corresponding values deduced by semiempirical expressions available in the literature and the correlation is satisfactory.

Keywords: Fibre reinforced concrete beams; Ultimate strengths; Stirrups; Steel fibres; Tests

1. Introduction

In seismic resistant reinforced concrete framed structures designed in agreement with the criterion of ''capacity design'', when severe actions occur a very dissipative collapse mechanism is required. Consequently, in order to allow attainment of the complete flexural bearing capacity in the critical regions, it is necessary to avoid the premature shear collapse that occurs when high values of shear stress are achieved and the shear reinforcement is not adequate. This is because shear collapse implies a sudden brittle failure that is very dangerous. For this reason, several codes [1–3] require a high percentage of transverse reinforcement in the critical regions. Many studies have been addressed to determine a suitable resisting mechanism and consequently to propose a theoretical model aimed at evaluating the mean value of the ultimate shear stress. These studies start from models based on flexure–shear interaction in beams without shear transverse reinforcement [4–6]; some of them propose a model taking into account the presence of the stirrups and the way in which they can interact with the beam and arch contributions [7].

Many reports published over the past 25 years have considered the possibility of utilizing fibre reinforced concrete by assigning the function of shear reinforcement to the fibres [8–24]; the achievable advantages are emphasized by ACI Committee 544 [25] and by RILEM TC 162-TDF [26]. Experimental investigations have shown that the inclusion of steel fibres in the concrete, using adequate quantities, improves the shear resistance because of: increase in tensile strength, delaying the formation and growth of cracks; smaller distance between fibres with respect to that between stirrups, implying greater effectiveness in the crack-arresting mechanism and better distribution of tensile cracks. In particular, Narayanan and Darwish [10] observe that the crack pattern that develops in fibre reinforced concrete beams subjected to shear is similar to that observed in the corresponding reinforced concrete beams with conventional stirrups. This remark comes from comparison between the performances of beams reinforced only with stirrups and of beams without stirrups but prepared with fibrous concrete using fibres in a percentage equivalent to that of

* Corresponding author. Tel.: +39-091-6568436; fax: +39-091-6568407.

E-mail address: lamendol@stru.diseg.unipa.it (L. La Mendola).

0958-9465/$ - see front matter © 2003 Elsevier Ltd. All rights reserved.
doi:10.1016/j.cemconcomp.2003.07.001

the stirrups in the shear span of the corresponding conventionally reinforced beams: the improvement in the ultimate mean shear strength is not significant, but the first crack shear strength increases noticeably. The same authors, in a subsequent paper [11] come to the conclusion that the fibres cannot entirely replace the conventional shear reinforcement when the structural elements are subjected to very high shear stress. However, the use of fibres reduces the severity of the failure mode, which can change from a brittle shear into a ductile flexural failure. This conclusion is found in most papers in which this subject is treated. They are often based on a large number of experimental tests, which are utilized to achieve an expression for predicting the shear strength share due to the fibres. This share is related to an improvement in the dowel action and in the arch action of the beam [8,10]. It can be related to the pullout resistance offered by the fibres crossing the cracked section, taking into account that the fibre length is less than that required to develop the ultimate tensile strength of the fibre itself. Several authors have proposed empirical expressions and analytical models to evaluate the contribution of fibres to the ultimate shear strength [9,10,12,14–17,20,22,24]; it can be observed that this contribution depends essentially on the volume fraction of the fibres, on their geometric characteristics and on the fibre-matrix interfacial bond that determines the resistance to fibre pullout.

A limited amount of experimental data is available in the literature concerning the shear behaviour of beams, in which coupled use of fibres and conventional transverse reinforcement is realized. In this paper an experimental investigation on 16 beams is described. Eight specimen types were prepared by considering two percentages of stirrups, two volume percentages of fibres and, in order to allow a more efficacious comparison, also beams in plain concrete with and without stirrups and beams in fibrous concrete without stirrups were prepared. The aim of the investigation, carried out by considering two different values of shear span for the two series of eight beams, consists of the evaluation of the improvement in the post-peak behaviour due to the presence of fibres and in particular to the coupled effect of fibres and stirrups. Therefore controlled displacement tests are carried out in order to record the complete load–deflection curve, allowing to deduce information about the dissipative capacity of the structural member up to rupture.

2. Experimental programme

2.1. Materials

The concrete used to prepare the beams was made from Portland cement type 42.5, sand, aggregate and water using the mix proportions given in Table 1. The maximum size of coarse aggregate (10 mm) was chosen in accordance with the RILEM TC 162-TDF recommendations [27]. Hooked-end steel fibres were used; they were joined together by a water soluble glue to ensure good dispersion in the concrete. The fibres had the following characteristics: length $L_f = 30$ mm; equivalent diameter $D_f = 0.5$ mm (aspect ratio $L_f/D_f = 60$); nominal tensile strength of 1115 MPa. Two volume percentages of fibres, $V_f = 1\%$ and 2% with respect to the volume of concrete, were used, equivalent to 80 and 160 kg/m^3 respectively. Since addition of fibres reduces the workability of the fresh concrete, a superplasticizer with a dosage of 1.5% by weight of cement was added to the mixes. In order to design the beams in the absence of shear reinforcement, knowledge of the compressive strength of the plain concrete described above was necessary. To this purpose three cylindrical specimens with diameter 100 mm and height 200 mm were cast. Moreover, to obtain more details on the strength and on the deformation capacity of the concrete, simultaneously with the preparation of the beams made of plain concrete and of fibrous concrete, six cylindrical specimens of the same dimensions were prepared in order to carry out three compressive tests and three indirect tensile tests for each type of concrete.

Table 1
Concrete mix design details

Cement (Portland 42.5)	450 kg/m^3
Sand	850 kg/m^3
Coarse aggregate ($d_a = 10$ mm)	1050 kg/m^3
Water	160 kg/m^3

The longitudinal reinforcement of the beams constituted of deformed bars with diameter 20 mm, bent at the ends to ensure a good anchorage condition, while the transverse reinforcement was realized by using deformed bars with diameter 6 mm. The steel bars in both cases were type $f_{yk} \geqslant 435$ MPa.

2.2. Beams

Eight types of beams, with different amounts of stirrups and/or fibres, were prepared. For each type, two beams with the same transverse reinforcement were prepared, in order to consider two different values of shear span, so as to evaluate the influence of this parameter on the shear–moment interaction phenomenon. All the beams had a rectangular cross-section of dimensions $b = 150$ mm, $h = 250$ mm and length of the span $L = 2500$ mm. The area A_s of the longitudinal reinforcement was designed to obtain, in the absence of specific shear reinforcement, a premature shear mode of failure. The ultimate moment of the beam, in the presence of shear, evaluated as the sum of the two contributions due

to beam and arch effects, is provided by the following expression [5]:

$$M_u = \left[0.83\xi\rho^{\frac{1}{3}}f_c'^{\frac{1}{2}}\frac{a}{d} + 206.9\xi\rho^{\frac{5}{6}}\left(\frac{a}{d}\right)^{-\frac{3}{2}}\right]bd^2 \quad (1)$$

in which $\rho = A_s/(bd)$ is the tensile reinforcement ratio evaluated with reference to the effective beam depth d, f_c' is the compressive concrete strength in MPa, a/d is the shear span-to-depth ratio, ξ is a function taking into account the aggregate size effect,

$$\xi = \frac{1}{\sqrt{1 + d/(25d_a)}} \quad (2)$$

with d_a maximum size of the aggregate.

The flexural capacity of the beam, calculated according to ACI Building Code recommendations [1], is expressed as

$$M_{fl} = bd^2\rho f_y\left(1 - \frac{\rho f_y}{1.7f_c'}\right) \quad (3)$$

with f_y the yield strength of the reinforcing bars.

Taking into account that the tensile reinforcement of the beams consists of two longitudinal deformed bars with diameter 20 mm, the relative flexural capacity M_u/M_{fl} with variation in the dimensionless shear span proves to be that shown in Fig. 1, in which the data necessary to construct the valley of diagonal failure [4] are also given. In particular, f_c' is obtained as the mean value of the cylindrical strength of the three specimens of plain concrete; f_y is the mean value obtained by the tensile test on three specimens of steel bar; the effective beam depth d is kept the same in all beams both in the presence and in the absence of stirrups, with a cover equal to 15 mm in the case of beams with stirrups, and 21 mm in the absence of stirrups. The M_u/M_{fl} versus a/d curve shows a minimum value corresponding to $(a/d)_c = 2.31$; this value of the a/d ratio is a "critical value" because it discriminates between two failure modes: for $a/d > (a/d)_c$ the beam mechanism governs and the failure is usually termed as a diagonal-tension (DT) failure; for $a/d < (a/d)_c$ the arch mechanism governs and the failure is usually termed as a shear-compression (SC) failure. The values of a/d relative to the two series of eight beams were chosen in order to obtain the two different failure modes, compatible with the limits of the testing setup arrangement for the experimental investigation: $a/d = 2.8$ for the series A and $a/d = 2.0$ for the series B.

When stirrups were used, two longitudinal bars with diameter 10 mm were inserted in the compressive region of the beam, in order to assure a good arrangement of the stirrups.

In Fig. 2 the different types of specimens investigated, by varying the transverse reinforcement with spacing $s = 200$ mm or $s = 60$ mm, are shown.

Each beam is marked with a letter followed by two indexes: the letter represents the shear span chosen for the test (A for $a/d = 2.8$ and B for $a/d = 2.0$); the numerical indexes that follow refer to the fibre percentage (0 in absence of fibres; 1 for $V_f = 1\%$ and 2 for $V_f = 2\%$) and to the stirrup reinforcement (0 in the absence of stirrups; 1 for $s = 200$ mm and 2 for $s = 60$ mm) respectively.

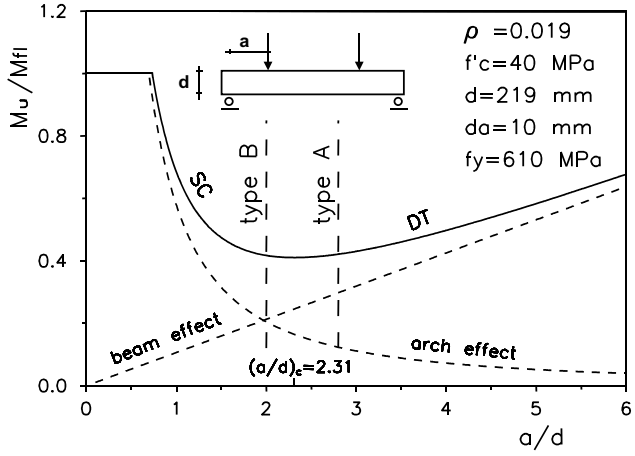

Fig. 1. Classification of beams based on Kani's valley.

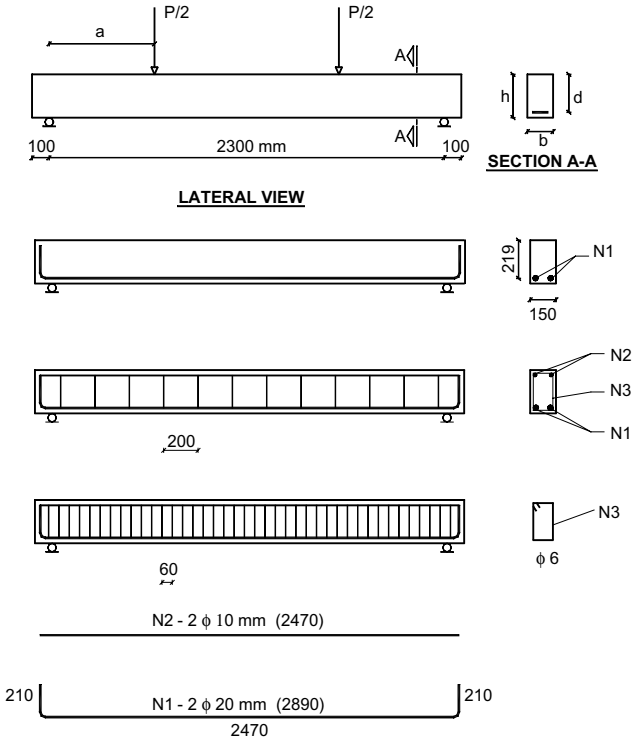

Fig. 2. Geometry and reinforcement details.

3. Material properties

3.1. Concrete

Three compressive tests were carried out for each type of concrete. A universal testing machine with controlled displacement, having a maximum load capacity of 600 kN was utilized. In order to minimize possible rotational effects due to not uniform distribution of the compressive load, a spherical joint was located between the loading jack of the machine and the plate in contact with the specimen. Fig. 3 shows the curves obtained as the mean of the results of three tests for each concrete type; only the curves for the mean of the results are represented, because the results obtained for each single test were very close to each other.

The normal stress σ was calculated as the ratio between the applied load and the nominal area of the cross-section. Considering possible different local deformations of the specimen, the strain ε was deduced as the mean value of readings of three LVDT's located in plan in such a way as to form an angle of 120° with one another, on a gauge length equal to 100 mm. They were placed in the middle part of the specimens, to ensure recording of deformations not affected by boundary condition effects. During the tests, the strain values recorded by the three LVDT's in the ascending branch of the σ–ε curves were very close to one another; in the post-peak branch, the maximum scatter of the different readings was 15%.

The curve relative to the plain concrete shows a quasi-elastic initial branch, followed by a nonlinear branch up to the maximum stress value at which cracking appears with very rapid propagation of cracks. This phenomenon does not allow valid recording in the post-peak branch. The curves for the fibrous concrete are very close to the one for the plain concrete in the ascending branch; but their post-peak branch is significantly different because of a more gradual microcracking process allowing more ductile behaviour. The mean values of the most important characteristics obtained from the tests carried out are contained in Table 2, in which f'_c is the maximum stress, ε_0 the corresponding strain value and E_c the initial tangent modulus.

Several papers show that the use of splitting-tension tests to determine improvement in the tensile strength due to the fibres is appropriate [9,10,13–15,19–21,28,29]. In particular, Nanni [28] dedicates his paper to this specific objective, providing experimental data to encourage wider acceptance of this test. In accordance with this suggestion three splitting-tension tests for each type of mix were carried out on cylindrical specimens. The results obtained are presented in Fig. 4 in terms of load–displacement diagrams for the different fibre percentages considered.

The curves show a remarkable increase in the peak with an increase in the fibre content and a sub-horizontal post-peak branch when fibres are used. The mean values of the maximum strength f'_t obtained from the

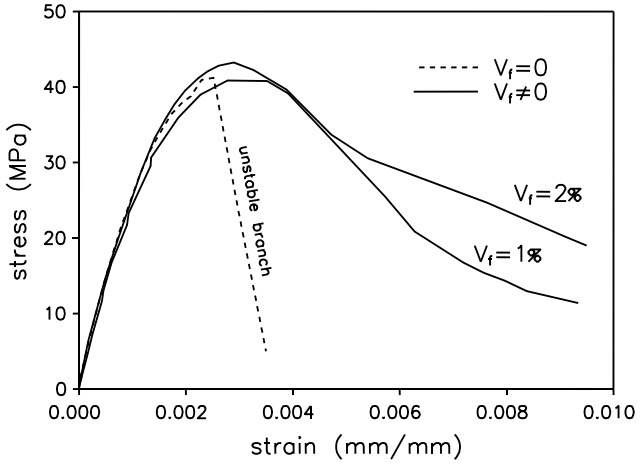

Fig. 3. Results of compression tests on plain and fibrous concrete.

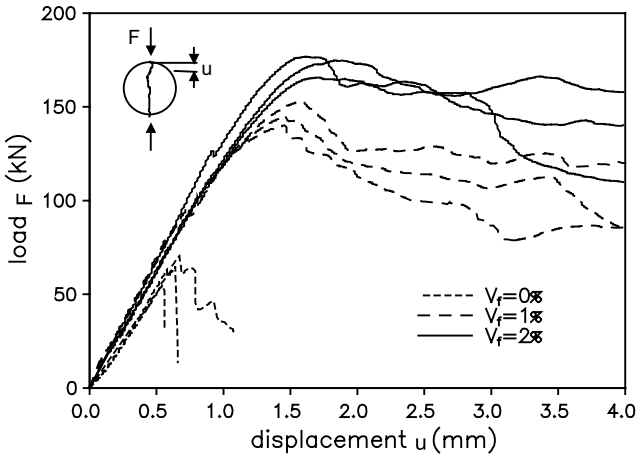

Fig. 4. Results of splitting-tension tests on plain and fibrous concrete.

Table 2
Properties of concrete mixtures

V_f (%)	f'_c (MPa)	$\varepsilon_0 \times 10^3$	E_c (MPa)	f'_t (MPa)
0	41.20	2.513	26 094	2.02
1	40.85	2.780	26 236	4.65
2	43.23	2.898	26 373	5.49

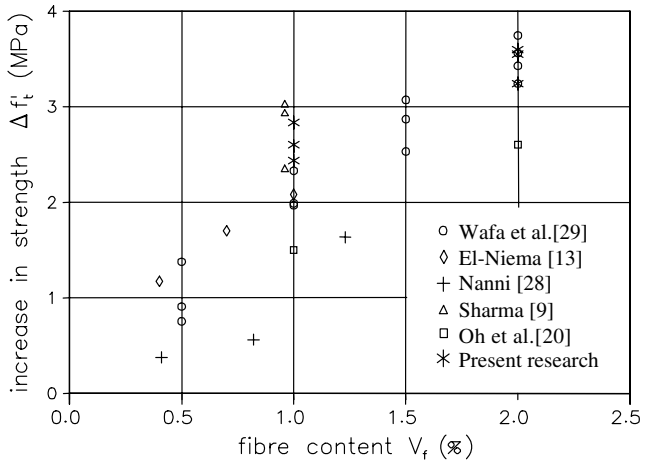

Fig. 5. Increase of splitting tensile strength f'_t with fibre content V_f.

three tests for each fibre percentage considered are contained in Table 2. Moreover, a comparison with some data present in the literature is shown in Fig. 5, in which results of tests relative to normal strength concrete and steel fibres with similar characteristics to those utilized in this investigation are represented. The ordinate indicates the increase in strength obtained as the difference between the values f'_t for the fibrous and plain concrete. It can be stressed that the splitting tensile strength increases more than twofold at a fibre volume of 2%, as also observed in [20,29].

3.2. Steel

To characterize the steel of the deformed bars with diameter 20 mm and diameter 6 mm, forming the tension reinforcement and the stirrups respectively, three tensile tests on specimens of 300 mm length for each type of bar were carried out. The same universal testing machine (with controlled displacement) used for the compressive tests was employed, with a load cell of capacity 600 kN for the bars of 20 mm diameter and a load cell of 120 kN for the bars of 6 mm diameter.

The characteristic values, evaluated from the mean σ–ε curves, can be assumed to be the following: Young's modulus $E_s = 232\,000$ MPa; yield strength $f_y = 610$ MPa for the longitudinal bar and 510 MPa for the bar constituting the transverse reinforcement.

4. Test arrangement and procedure

Tests on the beams were executed using the same testing machine with controlled displacement as used for the tests on the materials, with maximum capacity equal to 600 kN. The load P was applied via spherical joint attached to a rigid steel beam resting on the reinforced concrete beam by means of two steel cylinders. These cylinders make it possible to realize the shear span necessary for the tests by their different location. A load cell connected to a data acquisition system made it possible to record the actual load. The supports were provided by steel cylinders that ensures the absence of significant components of horizontal reactions during the test. These cylinders were placed on a very rigid steel beam that provided the reaction load (clean span $L_c = 2300$ mm).

During the test, carried out employing a displacement rate of 0.5 mm/min, the displacements were measured using three LVDT's: one placed in the section corresponding to the mid span in the lower part of the beam; the other two placed at the supports of the beam. The effective deflection of the beam at each displacement step was obtained by means of the value recorded at the mid span section decreased by the mean value of the displacements at the supports of the beam. The latter displacements, in all tests, showed linear variation with the applied load, and their values were between 4% and 6% of the deflection.

The results of all tests, carried out with monotonically increasing displacements, are shown and discussed in the next section.

5. Results and discussion

5.1. Beams without shear reinforcement

The beams prepared with plain concrete and without stirrups were tested for both shear spans, in order to verify the expected failure modes. The results obtained are shown in Fig. 6 in terms of P–δ curves, P being the total load transmitted by the testing machine and δ the deflection measured as specified before. Both curves show a reduced flexural capacity, as expected. In particular, it can be observed that: the beam A00 reaches the ultimate condition for $P_u = 81$ kN, corresponding to a value of $M_u = 24.834$ kN m; this moment value compared to M_{fl} calculated by using Eq. (3), in which $f_y = 610$ MPa and $f'_c = 41.2$ MPa ($M_{fl} = 69.583$ kN m), provides $M_u/M_{fl} = 0.357$ with respect to the theoretical value 0.423; the beam B00 reaches the ultimate condition for $P_u = 99$ kN and a reduced flexural capacity $M_u/M_{fl} = 0.312$ with respect to the theoretical value 0.418. Therefore, both experimental values prove to be lower than the expected values by 16% and 25%, respectively, but this occurrence is not very significant, considering that the results refer to a single test for each load condition. However, the pattern of the theoretical curve (Kani's valley) in Fig. 1 is confirmed, although it overestimates the actual values. Fig. 6 also shows the first cracking and the crack pattern at the end of the tests. In both cases the failure is characterized by formation of diagonal cracks. The pattern of the load–deflection

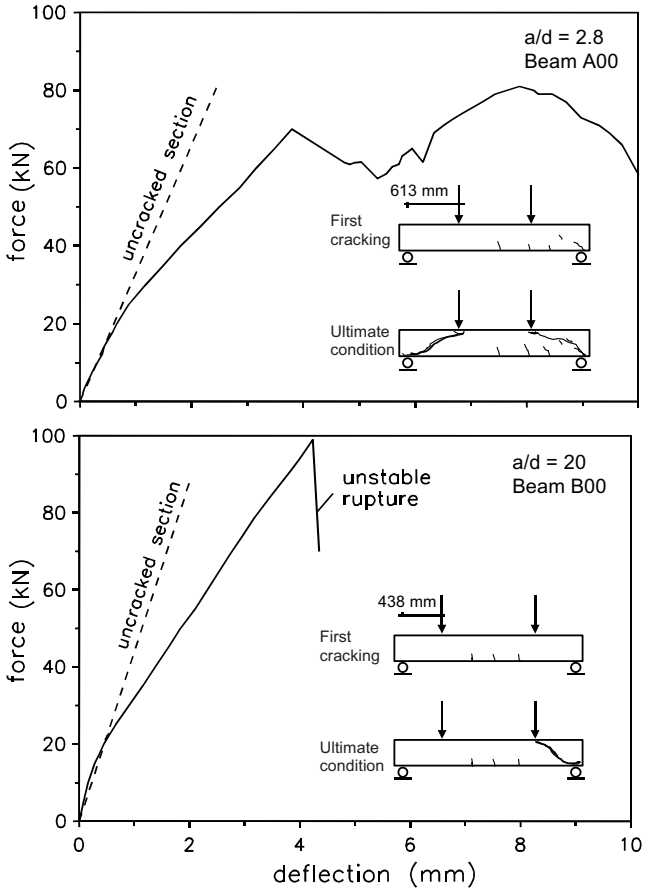

Fig. 6. Load–deflection curves for beams without shear reinforcement.

curves reveals what was observed during the tests: for beam A00 the beam effect prevails in the rupture mechanism and the failure is due to the overcoming of the tensile strength of the concrete, followed by inclined cracks that become unstable and extend up to the compressive zone; for beam B00 the arch effect governs the failure with diagonal cracking followed by concrete splitting along the predominant crack. For this reason, after the ultimate load is reached, rapid increase of the crack width appears, corresponding to a sudden loss of bearing capacity not allowing any significant recording in the post-peak branch of the curve. Finally in the same figure the straight lines corresponding to the initial theoretical elastic behaviour are shown. They are obtained by assuming that the cross-section remains uncracked and the concrete has the same elasticity modulus values in compression and in tension. Moreover, shear deformability is considered, assuming a Poisson's ratio equal to 0.2 in the evaluation of the shear elasticity modulus.

5.2. Beams with shear reinforcement

In this section the results obtained from the tests carried out on beams with shear reinforcement, constituted of stirrups and/or fibres, are presented. The load–deflection curves obtained from series A, with $a/d = 2.8$, are presented in Fig. 7. The curve relative to the beam without fibres and stirrups is also represented (Fig. 6) for an immediate comparison of the different responses. In the same diagram the theoretical value of the ultimate load $P_{fl} = 227$ kN, corresponding to the case in which the beam reaches the full flexural capacity ($M_u/M_{fl} = 1$), is indicated. The comparison of the curves shows that the addition of shear reinforcement in an adequate percentage can modify the failure mode: the change from a brittle shear into a ductile flexural failure mode is revealed by the ultimate load value (close to P_{fl}) and the post-peak curve, which in the first case is very steep, while in the second case it is almost horizontal.

In Fig. 8 the crack patterns at failure of series A beams are represented: it can be observed that the flexural failure mode (beams A02, A20, A21, A12) is characterized by cracks that appear progressively, allowing the beam to reach significant ductility. When brittle failure occurs (beams A00, A01, A10, A11), the cracks are more localized and most of them are located above and along the inclined line joining the support with the point at which the load $P/2$ is applied. The experimental investigation also showed that, when stirrups are included, they are subjected to large deformations, which can imply attainment of the yield limit, as was observed in [7]. On the other hand it is known that the use of stirrups improves the beam action by increasing: the dowel action, because of the support offered to longitudinal bars; the strength of the concrete teeth, due to an inclined compression field associated with the truss mechanism; the interlock strength, due to crack opening control. When the spacing between the stirrups is larger ($s = 200$ mm) as in the case of beam A01, rupture of the stirrup crossing the cracked section occurs; this phenomenon can be reduced by the inclusion of fibres, as found in beam A11.

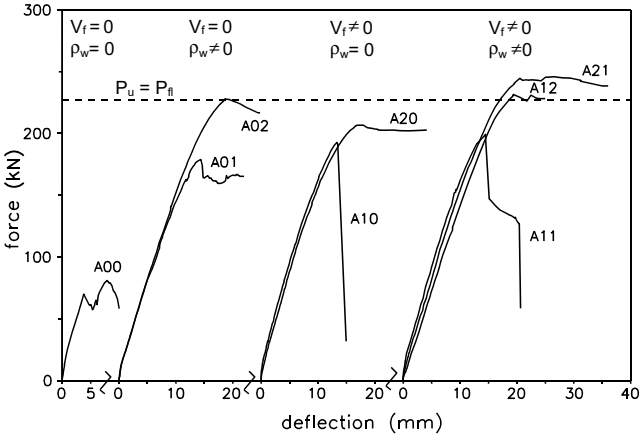

Fig. 7. Load–deflection curves for the series A beams ($a/d = 2.8$).

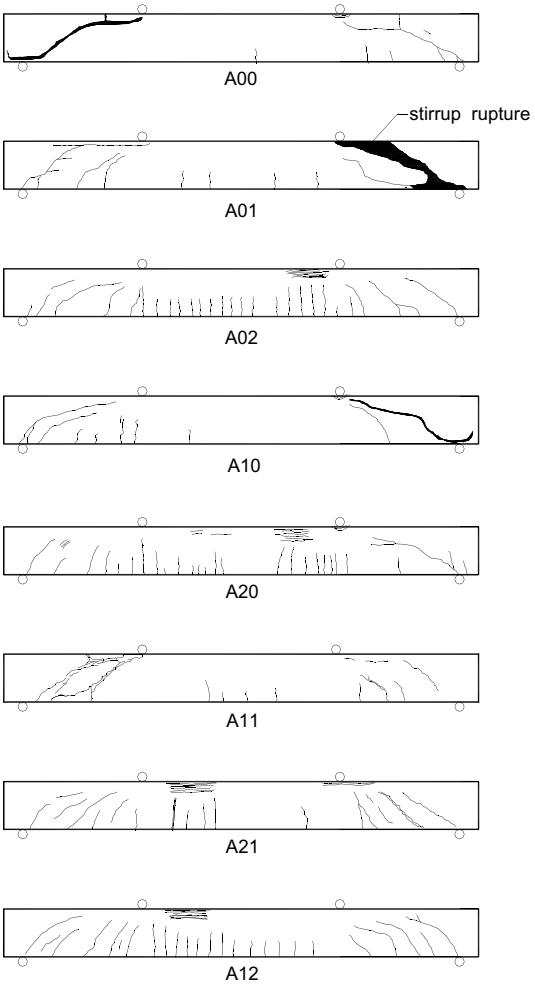

Fig. 8. Crack patterns at ultimate condition in the series A beams.

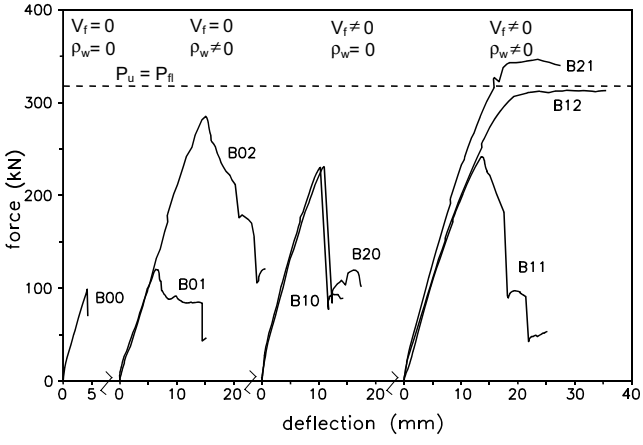

Fig. 9. Load–deflection curves for the series B beams ($a/d = 2.0$).

The load–deflection curves obtained by tests carried out on series B beams ($a/d = 2.0$) are shown in Fig. 9. A comparison with the results of beams in series A highlights more brittle behaviour. Only beams B12 and B21 were able to reach full flexural capacity. The others beams are characterized by brittle failure with diagonal cracking, in some cases involving rupture of stirrups. It can be observed that when the diagonal crack crosses several stirrups, the failure is progressive and the cracks are more spread, as shown by the comparison between the crack patterns of beams B01 and B02, represented in Fig. 10 together with those of the others types.

For series B beams, the use of stirrups is less effective with respect to what happens for the beams of series A; this is because the failure is governed by the arch effect, implying deformations that do not allow a meaningful development of the truss mechanism associated with the presence of stirrups.

By analysing the crack pattern of the beams at the end of the tests, it is possible to point out a correspondence between the cracking mechanism and the pattern of the load–deflection curves.

The experimental investigation carried out shows in general that the addition of fibres improves the structural response, both for the series A beams and series B beams, so much that an adequate content of fibres can

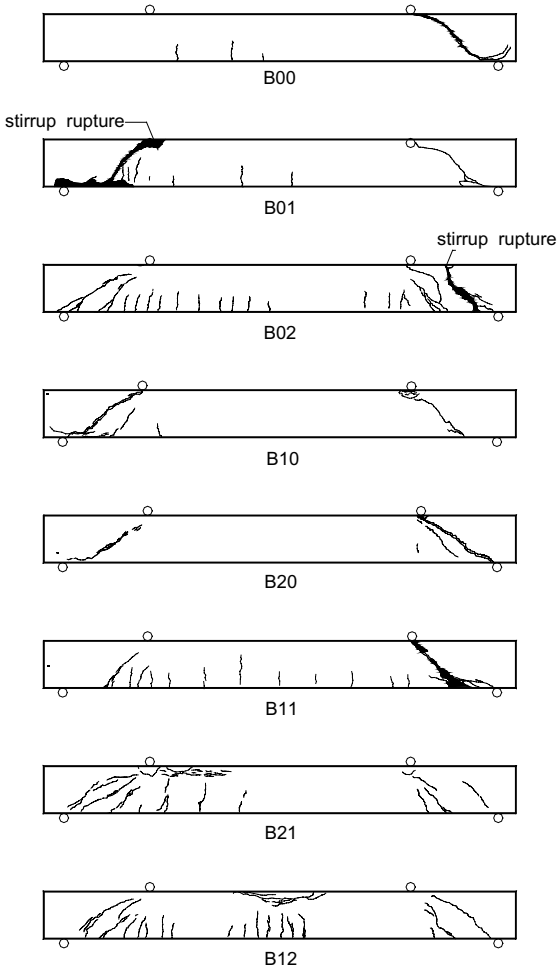

Fig. 10. Crack patterns at ultimate condition in the series B beams.

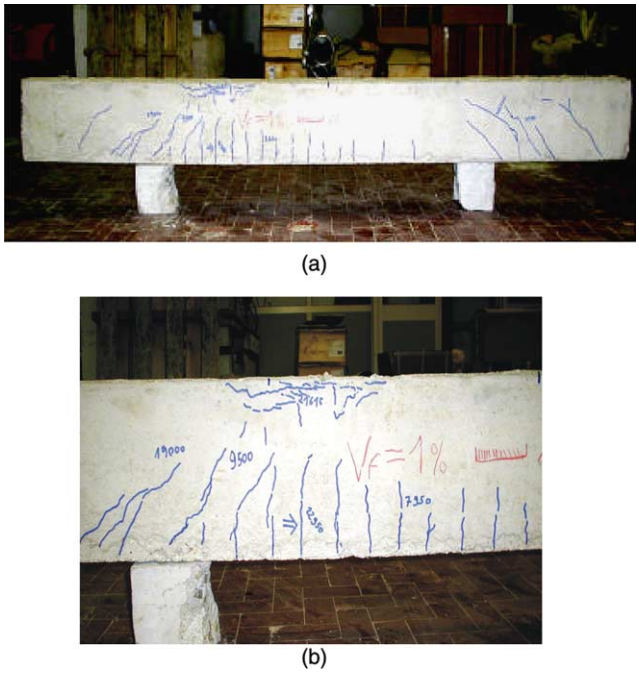

Fig. 11. Flexural failure of beam A12: (a) general view; (b) detail.

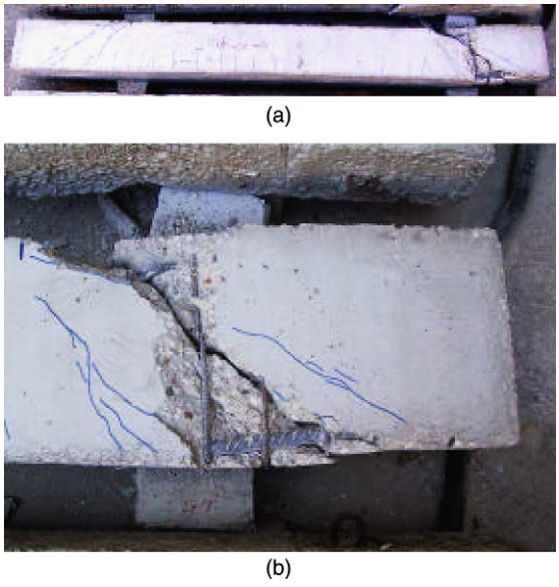

Fig. 12. Shear failure of beam B02: (a) general view; (b) detail.

change the failure mode, as happens for beam A11 and beam B11. The effectiveness of the fibres as shear reinforcement is more pronounced for the series A beams in which several cracks develop that significantly involve the pullout resistance of the fibres. This observation is confirmed by the comparison between the responses of beams without stirrups and with different amounts of fibres, $V_f = 1\%$ and 2%. Fig. 7 shows a considerable improvement in the response in the series A beams when fibres with volume percentage 2% are used rather than 1% (curves relative to beams A10 and A20), whereas Fig. 9 shows almost coincident curves for beams B10 and B20.

Finally, Figs. 11 and 12 show respectively the photographs at the end of the tests of beam A12, in which flexural failure has occurred, and of beam B02, in which shear failure with a crack involving rupture of the crossing stirrup has occurred.

6. Ultimate shear strength

In this section a comparison between the values of ultimate shear stress obtained by the experimental investigation ($v_u = V_u/(bd)$, being $V_u = P_u/2$) and the values deduced by using the expressions proposed in the literature is carried out. In particular, for the beams without specific shear reinforcement, the expression used to calculate the ultimate moment by Eq. (1) is utilized:

$$v_c = v_a + v_b = 0.83 \cdot \xi \cdot \sqrt[3]{\rho} \cdot \chi \tag{4}$$

with

$$\chi = \sqrt{f'_c} + 250\sqrt{\frac{\rho}{(a/d)^5}} \tag{5}$$

in which v_a and v_b are the shear stresses due to the arch and beam actions respectively. A third term must be added in Eq. (4) when stirrups are included as in Russo and Puleri [7]:

$$v_s = \frac{1.67\sqrt{f'_c}}{\chi}\rho_w f_{yw} \tag{6}$$

in which $\rho_w = A_w/(bs)$ is the stirrup ratio evaluated with reference to the spacing s and f_{yw} is the yield strength of the stirrups. Eq. (6), governed by the parameter $\sqrt{f'_c}/\chi$, takes into account the different contribution made by the stirrups in the case in which the failure mode is governed by the arch effect or by the beam effect. The comparison between observed and predicted values is given in Table 3.

For the beams made of fibrous concrete three different expressions proposed in the literature are used below for comparison with experimental results.

The contribution due to the fibres evaluated as proposed by Al-Ta'an and Al-Feel [12] consists of an empirical expression based on a regression analysis carried out on experimental data for 89 beams:

$$v_f = \frac{8.5}{9}kV_f\frac{L_f}{D_f} \tag{7}$$

in which k is a factor reflecting the fibre shape. For hooked fibres, like those utilized here, Al-Ta'an and Al-Feel propose the value $k = 1.2$. This value is adopted here. The contribution of the fibres is added to that

Table 3
Ultimate shear stresses for beams with plain concrete

Type	Observed v_u (MPa)	Predicted [Eqs. (4) and (6)] v_u (MPa)	Observed v_u/predicted v_u
A00	1.233	1.467	0.840
A01	2.723	2.605	1.045
A02	3.470	5.261	0.660
B00	1.507	2.031	0.742
B01	1.833	2.853	0.642
B02	4.340	4.772	0.909

The beam notation is as follows: A and B refer to the shear span–depth ratio; the first digit indicates the absence of fibres; the last digit refers to the percentage of stirrups.

Table 4
Ultimate shear stresses for beams with fibrous concrete

Type	Observed v_u (MPa)	Predicted [Eqs. (4), (6) and (7)] v_u (MPa)	Predicted [Eqs. (4), (6) and (8)] v_u (MPa)	Predicted [Eqs. (9) and (6)] v_u (MPa)	Observed v_u/mean of predicted v_u
A10	2.934	2.143	2.384	2.396	1.271
A20	3.145	2.853	3.335	2.829	1.046
A11	3.034	3.279	3.521	3.533	0.881
A12	3.526	5.932	6.173	6.185	0.578
A21	3.744	3.998	4.481	3.975	0.902
B10	3.503	2.706	2.947	2.607	1.272
B20	3.516	3.416	3.898	3.078	1.015
B11	3.678	3.527	3.768	3.427	1.029
B12	4.767	5.442	5.683	5.342	0.868
B21	5.276	4.248	4.730	3.909	1.228

The beam notation is as follows: A and B refer to the shear span–depth ratio; the first digit refers to the percentage of fibres; the last digit refers to the percentage of stirrups.

furnished by Eq. (4) for beams without stirrups and by Eqs. (4) and (6) in the presence of stirrups.

Swamy et al. [16] have proposed an expression to evaluate the contribution due to the fibres as a function of the average fibre-matrix interfacial bond stress τ:

$$v_f = 0.37\tau V_f \frac{L_f}{D_f} \tag{8}$$

in which τ is assumed equal to 4.15 as suggested in [10,14,22] for steel fibres, in the absence of specific pullout tests on the fibre reinforced concrete used in this investigation.

Finally, the empirical relation proposed in [9] is also utilized to determine the shear strength of fibre reinforced concrete beams:

$$v_c + v_f = k' f_t' \left(\frac{d}{a}\right)^{0.25} \tag{9}$$

in which k' is a constant equal to 2/3 because f_t' is the indirect tensile strength determined with the splitting-tension tests. For the beams with stirrups the contribution v_s provided by Eq. (6) is added.

In Table 4 the results obtained by using different expressions are contained; moreover, in order to calculate the ratio between the observed and predicted values the mean values furnished by the three expressions have been calculated.

The values contained in both tables are represented in the diagram in Fig. 13. It can be observed that the predicted values obtained by evaluating the contribution of fibres with different expressions present in the

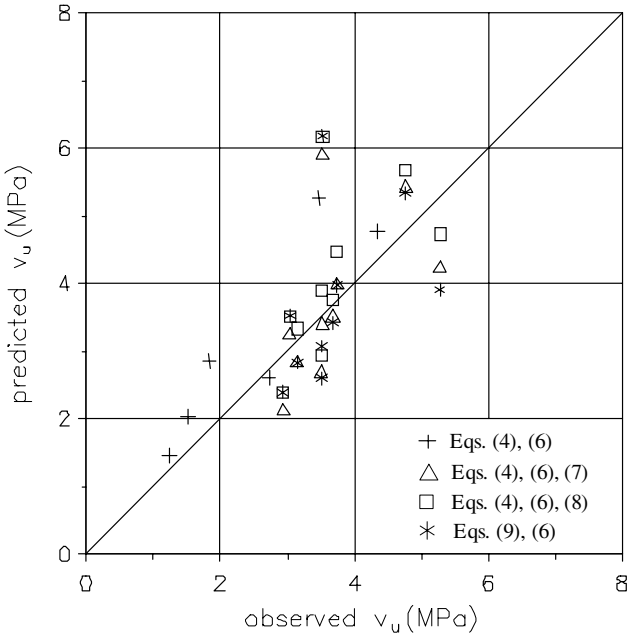

Fig. 13. Measured and calculated mean ultimate shear stresses.

literature are quite close to one another. The difference between the experimental results and the prediction, except for some cases, can be deemed acceptable, also considering the limited number of beams tested for each type. The more pronounced difference for beam A12 is probably due to the close spacing of the stirrups in relation to the fibre length used here, which in some cases can determine inadequate compaction of the concrete.

7. Concluding remarks

The experimental investigation presented here, carried out by displacement controlled tests on beams under combined actions of flexure and shear, shows the possibility of changing the failure mode, making it more ductile, by using fibre reinforced concrete.

The experimental results obtained confirm some remarks that other authors have also made, and precisely:

- during the tests, in fibre reinforced concrete beams a more progressive cracking process has been observed, with reduced crack widths;
- it is possible to obtain comparable performances in terms of ultimate strength by using steel fibres as shear reinforcement in an adequate dosage instead of stirrups, although a coupled use is more suitable because stirrups allow a greater deformation capacity beyond the elastic limit;
- the presence of fibres proves to be more efficacious in beams in which the failure in the absence of adequate shear reinforcement is governed by a beam effect.

Moreover, the load–deflection recording including the post-peak branch, allows one to draw the following conclusion:

- the inclusion of fibres can modify the brittle shear mechanism into a ductile flexural mechanism, thus allowing a larger dissipation of energy, as can be seen by observing the crack pattern and the load–deflection curves.

Acknowledgement

The financial support of the University of Palermo (Italy) and the Ministry for Education, Universities and Research (MIUR, Italy, PRIN 2002) is gratefully acknowledged.

References

[1] ACI Committee 318. Building code requirements for reinforced concrete (ACI 318-83. Detroit: American Concrete Institute; 1983. 111p.
[2] Standards New Zealand. Code of practice for general structural design and design loadings for buildings (NZS 4203:1992). Wellington, 1992.
[3] prEN 1998-1. Eurocode 8: Design of structures for earthquake resistance. Part 1: General rules, seismic actions and rules for buildings. European Committee for Standardization (CEN), Brussels, 2001.
[4] Kani GNJ. Basic facts concerning shear failure. ACI J Proc 1966;63(6):675–92.
[5] Bažant ZP, Kim JK. Size effect in shear failure of longitudinally reinforced beams. ACI J 1984;81(5):456–68.
[6] Russo G, Zingone G, Puleri G. Flexure–shear interaction model for longitudinally reinforced beams. ACI Struct J 1991;88(1):60–8.
[7] Russo G, Puleri G. Stirrup effectiveness in reinforced concrete beams under flexure and shear. ACI Struct J 1997;94(3):227–38.
[8] Swamy RN, Bahia HM. Influence of fiber reinforcement on the dowel resistance to shear. ACI J 1979;76(2):327–55.
[9] Sharma AK. Shear strength of steel fiber reinforced concrete beams. ACI J Proc 1986;83(4):624–8.
[10] Narayanan R, Darwish IYS. Use of steel fibers as shear reinforcement. ACI Struct J 1987;84(3):216–27.
[11] Narayanan R, Darwish IYS. Shear in mortar beams containing fibres and fly ash. J Struct Eng ASCE 1988;114(1):84–102.
[12] Al-Ta'an SA, Al-Feel JR. Evaluation of shear strength of fibre-reinforced concrete beams. Cem Concr Compos 1990;12(2):87–94.
[13] El-Niema EI. Reinforced concrete beams with steel fibers under shear. ACI Struct J 1991;88(2):178–83.
[14] Ashour SA, Hasanain GS, Wafa FF. Shear behavior of high-strength fiber reinforced concrete beams. ACI Struct J 1992;89(2):176–84.
[15] Tan KH, Murugappan K, Paramasivam P. Shear behaviour of steel fiber reinforced concrete beams. ACI Struct J 1992;89(6):3–11.
[16] Swamy RN, Jones R, Chiam ATP. Influence of steel fibres on the shear resistance of lightweight concrete T-beams. ACI Struct J 1993;90(1):103–14.
[17] Di Prisco M, Romero JA. Diagonal shear in thin-webbed reinforced concrete beams: fibre and stirrup roles at shear collapse. Mag Concr Res 1996;48(174):59–76.
[18] Adebar P, Mindess S, St-Pierre D, Olund B. Shear tests of fiber concrete beams without stirrups. ACI Struct J 1997;94(1):68–76.
[19] Furlan JrS, de Hanai JB. Shear behaviour of fiber reinforced concrete beams. Cem Concr Compos 1997;19(4):359–66.
[20] Oh BH, Lim DH, Yoo SW, Kim ES. Shear behaviour and shear analysis of reinforced concrete beams containing steel fibres. Mag Concr Res 1998;50(4):283–91.
[21] Campione G, La Mendola L, Zingone G. Shear resistant mechanisms of high strength fibre reinforced concrete beams. In: Brebbia CA, Oliveto G, editors. Earthquake resistant engineering structures ERES II. Catania: WIT Press; 1999. p. 23–32.
[22] Khuntia M, Stojadinovic B, Goel SC. Shear strength of normal and high-strength fiber reinforced concrete beams without stirrups. ACI Struct J 1999;96(2):282–9.
[23] Campione G, La Mendola L, Zingone G. Flexural-shear interaction in light strength fibre reinforced concrete beams. In: Rossi P, Chanvillard G, editors. Fibre-reinforced concretes (FRC) BEFIB'2000. Proc of the Fight Int Rilem Symp, Lyon, France, 2000. p. 451–60.
[24] Noghabai K. Beams of fibrous concrete in shear and bending: experiment and model. J Struct Eng ASCE 2000;126(2):243–51.
[25] ACI Committee 544. Design considerations for steel fiber reinforced concrete. ACI Struct J 1988;85(5):563–80.
[26] Rilem TC-162-TDF: Test and design methods for steel fibre reinforced concrete. Mater Struct 2000;33(226):75–81.
[27] Rilem TC-162-TDF: Test and design methods for steel fibre reinforced concrete. Mater Struct 2001;34(1):3–6.
[28] Nanni A. Splitting-tension test for fiber reinforced concrete. ACI Mater J 1998;85(4):229–33.
[29] Wafa FF, Hasnat A, Tarabolsi OF. Prestressed fiber reinforced concrete beams subjected to torsion. ACI Struct J 1992;89(3):272–83.